A Power Hardware-In-the-Loop Laboratory Setup to Study the Operation of Bidirectional Electric Vehicles Charging Stations

A Power Hardware-In-the-Loop Laboratory Setup to Study the Operation of Bidirectional Electric Vehicles Charging Stations

Andrea Mazza, Enrico Pons, Ettore Bompard
Dip. Energia & Energy Center Lab
Politecnico di Torino
Torino, Italy
name.surname@polito.it

Giorgio Benedetto
Dip. Energia
Politecnico di Torino
Torino, Italy
giorgio.benedetto@studenti.polito.it

Paolo Tosco, Marco Zampolli, Rémi Jaboeuf
Research, Development and Techn. Innovation Dep.
Edison SpA
Milano, Italy
name.surname@edison.it

***Abstract*—The needs for decarbonizing the entire energy system calls for new operational approaches in different sectors, currently (almost) fully dominated by fossil fuels, such as the transports. In particular, the decarbonization of the people transport, based on the implementation of Battery Electric Vehicles, may have a twofold benefit, because of (i) the reduction of local and global emissions, and (ii) the role that the Battery Electric Vehicles can have in supporting the operation of grids in case of large share of non-dispatchable renewable energy sources. This papers aims to investigate, through a Power Hardware-In-the-Loop laboratory setup, the impact of the Vehicle-to-Grid and Grid-to-Vehicle paradigms on a Low Voltage grid portions serving as microgrid an energy community. The results show that the grid losses, if not taken into account, can cause a wrong evaluation of the impact of the Battery Electric Vehicles on the grid.**

***Index Terms*—Vehicle-to-Grid, Grid-to-Vehicle, Real-Time Simulation, Power Hardware-in-the-Loop, Low-Voltage system**

I. Nomenclature

ΔV*: Voltage drop.*

P_{ist}*: Total ctive power of the total load.*

S*: Total apparent power.*

V_{sim}*: Single phases voltages the ending node.*

v_j*: voltage on the phase* j*.*

I*: Total load current.*

II. Introduction

A. Motivation and background

1) Energy transition: The decarbonisation process and the electrification of consumption are bringing new challenges to the electricity network. On the one hand, renewable energy sources (RES) are penetrating more and more in the energy generation mix, so new strategies are being developed, thanks also to the active involvement of consumers (prosumers), trying to improve the quality of the electricity service even in cases of emergency [1]. Since 2019 the sale of electric vehicle (EV) has grown and the total sales are expected to grow at steeper rate to 11.2 million in 2025 and 31.1 million by 2030 [2]. This could lead to the increasing of the total load. In the studies [3] and [4] some projections of the increasing electricity demand are reported. As a result the major concern is the effect it will have on the load profile of the network and as a consequence the impact on the medium and low voltage distribution grids [5] and [6]. More power withdrawn may also cause the distribution transformers overload. The overloads can increase the ageing of the transformers so the evaluation of the transformers load will be necessary.

2) Opportunities: V2X and V2G: The primary objective of an electric vehicle charging station (EVCS) is charge the car battery. However a bidirectional charging station can provide some others additional services known as Vehicle to X (V2X) operations. Indeed, the vehicles can interact with the charging infrastructure at various level, an example is the vehicle to home (V2H) where the car can provide energy to the house. Secondly the well known vehicle to grid (V2G) where the cars can inject energy into the distribution grid, contributing to the ancillary services market. Some examples of the services that the V2G may provide are: (i) *Fast Frequency Regulation Service*, because requiring high power for relatively short time, usually 10-15 minutes [7]; (ii)*Voltage support*, with V2G can inject or absorb reactive power in order to maintain the grid voltage, and (iii)*Peak shaving*, with EVs discharging helping during the peak power demand.

B. Contributions and Organization

For the above mentioned reasons and to exploit the new opportunities, the development of advanced management systems is being more and more important for power networks. In this context, the deployment of new systems requires reliable

and repeatable tests and validations before being actually implemented. To achieve power network simulations as close as possible to the real world, the Real-Time simulation (RTS) will be used as the most efficient and reliable way to achieve all these requirements. With this method the impact of a EVCS group on the distribution network will be evaluated in terms of voltage profile on the distribution line, power losses and power factor of the wallboxes (WBs) aggregate. The use of a Real-Time platform allows the Power Hardware-in-the-Loop (PHIL) configuration to be implemented. Real-time simulation with PHIL has been chosen, instead of performing a steady state study as in [8], for two reasons:

- *Temporal granularity of losses*: The value of the losses is updated at each step of the simulation calculation and it is therefore possible to evaluate the management of the plant in real time.
- *Distortion introduced by a specific hardware*: the integration of power electronics, such as those found in WBs, causes harmonic distortion of the injected current and, consequently, of the voltage at the various nodes of the network. Firstly, the presence of these harmonics results in higher losses and voltage drops than in the ideal case. These aspects are difficult to estimate through the analysis of the system by means of the backward forward sweep (BFS) algorithm. The PHIL configuration allows to the real object (i.e., the WB) to inject distorted currents into the simulated network. In this way is it is easy to estimate the harmonic impact of the electrical quantities through simple voltage and current measurements in the simulation. Secondly, as the WB is inserted *In-the-Loop*, the harmonic distortion of the currents causes harmonic distortion on the voltages at the WB input. In order to evaluate the effect on the network of a specific hardware the PHIL Real-Time approach seems the most suitable.

III. Real-Time Simulation and Power Hardware-in-the-Loop configuration

A. Real-Time simulation tasks

Simulation of electrical power systems allows to solve real-world problems in a safe and repeatable way. There are two different types of simulation to refer to: the offline simulation and the online simulation [9]. In offline simulations the time required to solve all equations and functions that define the entire system could exceed the time-step; in this configuration both fixed and variable step can be adopted. In online simulation, all the calculations are accomplished during the time-step, which must be properly fixed, if the time required exceed the fixed step an overrun occurs. This latter type of simulation is better known as RTS: the fundamental principle on which an RTS is based is the reproduction of the behavior of a physical system through the execution of its computer-based model at the same speed as actual time, so that each advancement in the simulation time is synchronous to the advancement of the real time (1:1 ratio with the wall-clock), in this way the dynamic contingency is guaranteed.

The main advantage of Real-Time simulation is the possibility of replacing physical systems with virtual systems (models), but being able to insert external Hardware devices to be tested (DUT) in the simulation: this opportunity can mainly be achieved through the Hardware-in-the-Loop (HIL) and PHIL configuration. This allows users to perform realistic closed loop tests without the need to test real components [10]. While HIL refers to setups with low voltage signal connection, PHIL can be employed for higher power testing. PHIL simulation requires the creation of a virtual power interface between the RTS and DUTs. Typically, the power interface involves power amplifiers (voltage and/or current) and sensors [9], as shown in Fig. 1.

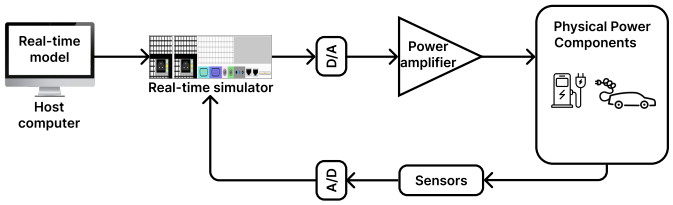

Fig. 1. PHIL simulation concept

PHIL can be useful for testing the impact of new technologies on large-scale grids in Real-Time, in a laboratory environment, and in a reliable and repeatable way. The PHIL concept is already proven and adapted in a larger number of application and some examples are reported in literature. In [11] a PHIL testbed is designed to model and test grid-connected battery energy storage systems in power system application. In [12] the PHIL simulation is used to validate two commercial photovoltaic inverters. In [13] two of the most popular variable-speed wind turbines are studied: the doubly-fed induction generator with partial-scale power converter and the permanent-magnet synchronous machine with full-scale power converter. In [14] a Real-Time simulation model and a PHIL simulation method of a Proton-exchange membrane (PEM) fuel cell stack system for emulating its electrical dynamics has been presented. Regarding specifically the charging systems of electric vehicles, in [15] is presented a comprehensive small signal model capable of describing the dynamics of a PHIL testbed developed for evaluating grid-connected EV chargers and, to conclude, in [16] a PHIL demonstrator is developed for the purpose of studying the impact of Electric Vehicle charging on low voltage distribution grids.

B. Interfacing DUT in PHIL simulation

The connection between simulation and the DUT is established with the interface algorithms. Interface algorithms provide the means of relating simulated voltage and currents at the point of coupling between the RT simulator and the DUT to the measured voltage and current of the PHIL amplifier. This element is critical for the stability and accuracy of the PHIL simulation [17]. There are some possible configurations as reported in [10], [17] and [18]: the one used in this work

is the the ideal transformer model (ITM) interface algorithm. This interface type is the simplest and straightforward method to connect the hardware side to the simulation, in PHIL applications the power amplifier receives the reference voltage signals from the real time simulator and provides power to the DUT [10]. In the meantime the current sensors measure the current signals on the hardware and feed them back to the real time simulator with an ideal current generators setup. Fig. 2 shows the PHIL implementation scheme of the ITM algorithm with the part related to the physical hardware components highlighted in blue.

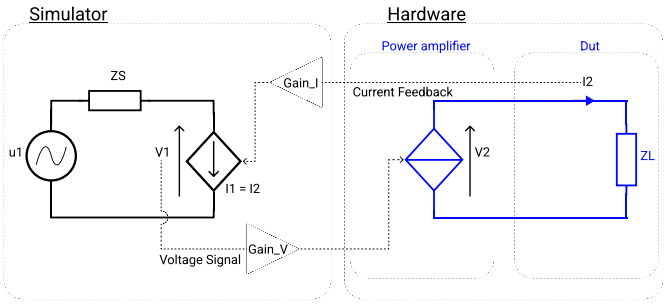

Fig. 2. PHIL Implementation scheme

C. Laboratory layout

This work was conducted in the G-RTS Lab at the Energy Center of the Politecnico di Torino (PoliTo), during a joint collaboration between PoliTo and Edison. G-RTS Lab, is an internationally interconnected lab for Real-Time simulation. It is active in studying the role of electricity in energy transition, as well as new smart grids and super grids for electricity. The activities of the G-RTS Lab are integrated into the Energy Center Lab (EC-Lab), where interdisciplinary studies related to different energy sectors (e.g., electricity, gas and heat) can be studied entirely. The facility is composed by two different Real-Time simulation platform with more computing cores available and the possibility to perform simulation in time domain as well as in phasor domain, power amplifiers from 20 to 60 kVA and a large number of hardware devices, e.g., a battery emulator, a photovoltaic system emulator, a load emulator, a resistive load and an electric vehicle charging station connected to an electric vehicle. The devices used for the presented test cases were a real time simulator, a linear amplifier, the charging station and the car and described below

Real time simulation platform.
The role of the RT simulator is essential to interface physical hardware components with a simulation environment, i.e., Simulink/Simscape in the performed tests. In order to guarantee a proper connection, the computation time (Ts) should be carefully chosen, the smaller time step, the smaller is also the introduced error, since the network solution is only calculated at discrete equidistantly spaced simulation time points [19].

Power amplifier.
The used power amplifier is a linear amplifier, four quadrants 21 kVA (7kVA per phase) that can be operated both in AC (three-phase) and DC. A linear amplifier has been chosen because this type of amplifier has very high dynamic performance. The short time delay introduced enables the use of simpler interface topology and less instability issues.

Charging station and electric vehicle.
The car used is a Nissan Leaf, which has a $62\,\mathrm{kW\,h}$ battery and uses the DC CHAdeMO plug, the only communication protocol that supports V2G operation and has standard libraries ready to implement. Of course the results obtained from the tests will be replicable with other connection protocols. The charger under test has a three phase supply with maximum charging and discharging power equal respectively to $11\,\mathrm{kW}$ and $10\,\mathrm{kW}$. A scheme of the laboratory setup is visible in the Fig. 3.

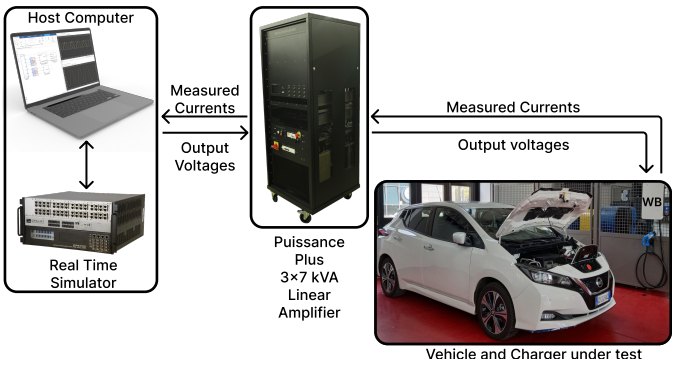

Fig. 3. Laboratory Layout

D. Real time simulation structure

With respect to a standard offline simulation, the model used to perform the test on the network is based on the OPAL-RT technology to exploit the Simulink simulation tools, with in addition some blocks from the simulation platform libraries following the documentation [20]. Therefore the compatibility between the model and the hardware has been guaranteed. In more detail the top level model has to be correctly set according to the simulator capabilities with each subsystem assigned to a computational core of the simulator. Moreover, the integration time step of the simulation was set to $50\,\mu\mathrm{s}$ in order to guarantee reliable results and a sufficient idle time to not generate computational overruns.

IV. Network Layout

A. Medium voltage network Layout

The chargers group is connected to a terminal node of one of the medium voltage (MV) line of the emulated distribution network. The medium voltage side is modeled on real data provided by Turin DSO, the wallbox group is then ”installed”

at the terminal node of the Brenta feeder. In Fig. 4 a simple representation of the electrical grid is given, each node represents a medium voltage to low voltage substation.

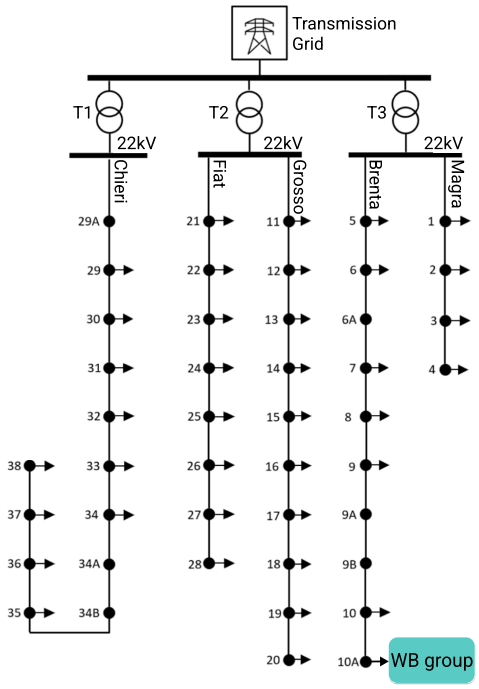

Fig. 4. Distribution network layout.

B. Microgrid Layout

The analysed microgrid would emulate a storage plant constituted by electric vehicle battery chargers, which have the capability to work in vehicle to grid mode in order to supply the energy needed to be part of the ancillary services market. The first tested layout is constituted by 5 groups of 4 chargers that can be independently switched on or off, to guarantee $200\,\mathrm{kW}$ of injected power. The tests have been conducted on a single real charger, so each group contributes to the total load multiplying the real measured currents, fed back into the simulation, by a gain of four. All of them are connected to the medium voltage section with a three phase low voltage line and a single transformer. This configuration allows to lower the cost of the components in a real application. The resin transformer has a nominal power equal to $315\,\mathrm{kV\,A}$, while the line has a cross section of $240\,\mathrm{mm}^2$. In Fig. 5 the layout of the low voltage section is showed.

V. Results

The main purpose of the performed tests is to understand the magnitude of the impact of wallboxes group on the low and medium voltage network in different load conditions in order to evaluate if a similar storage power plant could be connected to the real distribution grid. The tests are centered on the Brenta MV line which is connected to the tested load and the Magra one because is supplied by the same medium voltage to low voltage (MV/LV) transformer. The electric quantities

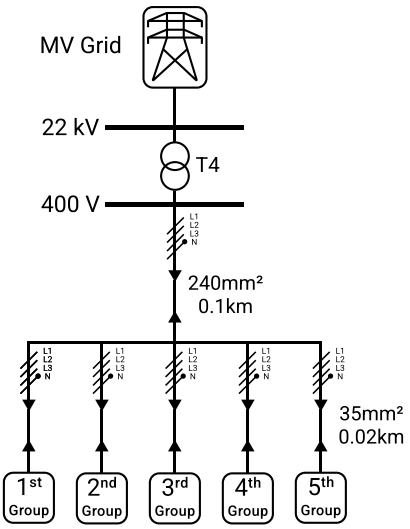

Fig. 5. Microgrid layout.

are measured in different points on two medium voltage distribution feeders, as showed in Fig. 6, and acquired for a short period of time in regime conditions, i.e. three seconds, to represent a snapshot of the worst working conditions. At the end of the Brenta feeder, the WB is highlighted in blue to distinguish the real tested hardware from the simulated environment (in black).

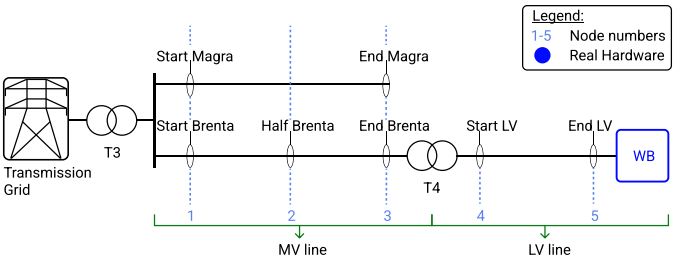

Fig. 6. Measurement points position

A. Voltage Profile

The connection of 20 simulated electric vehicles might exert an adverse effect on the existing power grid, both in grid to Vehicle (G2V) and V2G operations, especially when coincides with daily peak load at distribution level. One of the first indicator of the impact of the EVs on the grid is the voltage level along the distribution feeder.

Fig. 7 shows the obtained voltage profile of the tested section of the network, as expected the voltages are higher during V2G operation and lower in G2V, while in stand-by mode (used as a benchmark) the impact of the load on the medium voltage feeder is negligible. Some interesting observations can be made, first of all, from the pictures and briefly from Table I, is clearly visible how the impact of the load on the voltage level of both the medium voltage lines is negligible during the three working cases. Only while all the 20 wallboxes are charging a 1% difference, on the terminal

TABLE I
VOLTAGE LEVELS

Measurement points	Voltage Level (p.u.)		
	G2V	***V2G***	***Stand-By***
Start Magra-Brenta (1)	0.97	0.97	0.97
End Magra (3)	0.95	0.95	0.95
Half Brenta (2)	0.94	0.94	0.94
End Brenta (3)	0.93	0.94	0.94
Start LV (4)	0.91	0.96	0.94
End LV (5)	0.89	0.98	0.94

node of the medium voltage feeder, is present with respect to the other use cases. Secondly the 10% of maximum tolerance on the voltage level is exceeded on the terminal node of the low voltage line, during the charging procedure, indeed, the voltages are lower than $206\,\mathrm{V}$ rms, and can cause some problems to some hypothetical other loads connected on the same node. Moreover such a low voltage value caused in some occasions the end of the charging operations by the wallbox despite the minimum voltage requested from the hardware was lower. Furthermore the internal converter of the charging station tries to control itself as a constant power load, in this case if the voltages tend to decrease the currents absorbed will increase leading to higher power losses on the low voltages cables.

A comparison with a steady state theoretical approach for voltage drop calculation has been done on the low voltage line. The theoretical approximated voltage drop has been calculated as:

$$\Delta V = \sqrt{3} I (R cos\phi + X sin\phi) \tag{1}$$

where I is the line current, R is the line resistance and X the line reactance. The current value used is the fundamental component of the phase current, while the voltages used to evaluate the ending voltages are the values measured upstream of the low voltage line. The voltage at the end of the line, calculated with this approach, is equal to $206.61\,\mathrm{V}$. The value simulated in real-time with PHIL is equal to 0.89 p.u. which is equivalent to $205.54\,\mathrm{V}$; such a non negligible difference could be explained by the presence of current harmonics, that are not considered in the analytical calculation.

B. Power losses

Because the energy accounted from the DSO is not the nominal injected power, but the power measured on the connection point, the power losses through the MV/LV transformer and low voltages lines have been evaluated. In this way it is possible to evaluate the profitability of the presented plants and, if necessary, to oversize some components like the low voltage cables and transformer. To take in account the power losses caused by the frequency components higher than the fundamental, the waveforms of voltages and currents on the measurement points have been collected and the instantaneous active power in each point was computed. In Table II are briefly reported the power losses through the components of the microgrid. As expected in G2V operation the power losses are slightly higher than in V2G operations.

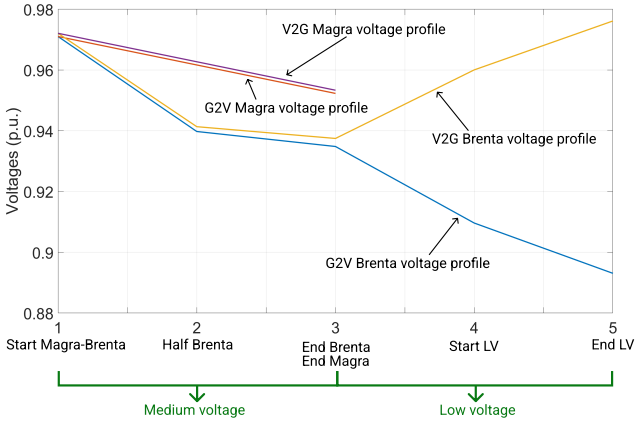

Fig. 7. 20 charge wallboxes voltage profile

TABLE II
POWER LOSSES

Component	Losses %	
	G2V	***V2G***
MV/LV transformer	1.68	1.566
LV line	1.578	1.349
LV line + MV/LV transformer	3.231	2.893

The measured losses then should be summed to the conversion losses, so the requested power on the connection point will be lower than the power sent by the converters so it is important to asses the total losses.

C. Power Factor

As reported in [21] the charging stations should provide a power factor higher than 0.9 when the output of the converters is over the 50% of the rated output power. In order to know if this request is met, the power factor of the wallboxes has been measured in G2V and V2G operations in different points of the microgrid to evaluate the impact of the lines on the power factor of the converters when they absorb or inject their maximum power. To retrieve the value of the power factor, the instantaneous waveforms of currents and voltages were used, than the active and apparent powers were calculated as:

$$P_{ist} = v_1 * i_1 + v_2 * i_2 + v_3 * i_3 \tag{2}$$

$$S = V_{sim} * I * 3 \tag{3}$$

$$cos\phi = P_{ist}/S \tag{4}$$

from the 3, the power factor, that include the contribution of the disturbances, has been retrieved with 4. The results are then reported in Table III.

As visible the power factor is lower than the nominal value of a single charger, which is controlled to be almost equal to 1, as tested in different load conditions. We can conclude that the lower value is due to the inductive components introduced by the low voltage lines. In Table III the stand-by power factor is also reported. Indeed, a consideration needs to be done on

TABLE III
POWER FACTOR

Measurement points	Power factor		
	G2V	***V2G***	***Stand-By***
End Brenta (3)	0.93	0.953	0.362
Start LV (4)	0.954	0.938	0.417
End LV (5)	0.956	0.935	0.417

the stand-by operations. The total power withdrawn in stand-by could be not negligible in a real application with an high number of EVCS connected, and such a low value of the power factor could lead to economic penalties from the energy authority.

CONCLUSION

High voltage deviations were observed from the nominal value, due to the high power withdrawn or injected in the low voltage side. Indeed, the voltages at the end of the low voltage side were lower than the limits in the G2V case. Due to the high power withdrawn also the power losses on the MV/LV transformer and on the low voltage lines are not negligible with a total value of 3.2% in G2V operations and 2.9% in V2G. These values, have to be summed to the conversion losses of the wallboxes, increasing the total losses. The voltage profiles presented and the calculation of losses take into account the harmonic contribution of the distorted current injected into the grid by the WB. Please note that, through the presented layout, these aspects can be evaluated in a simple way by measuring the electrical quantities through the simulation without the need to implement harmonic load flow algorithms as in the steady state case. In order to enhance the effciency of the low voltage microgrid it is worth to consider to oversize the MV/LV transformer and the low voltage lines. With the same configuration also the power factor has been evaluated, indeed, the power factor of the single unit is controlled to be almost equal to one, but the value of the aggregated needs to be measured. At full load, both for G2V and V2G, the power factor is higher than the limit (0.9), but lower than 1 due to the low voltage lines and the disturbances injected from the converters. Moreover the value in stand by is really low for the total load and if we consider an higher number of chargers this value could represent an issue, because the total stand by power withdrawn is not negligible, and some penalties could be applied.

REFERENCES

[1] G. Chicco, A. Ciocia, P. Colella, P. Di Leo, A. Mazza, S. Musumeci, E. Pons, A. Russo, and F. Spertino, *Introduction—Advances and Challenges in Active Distribution Systems*. Cham: Springer International Publishing, 2022, pp. 1–42.

[2] Deloitte. Deloitte insights. [Online]. Available: www2.deloitte.com/uk/en/insights/focus/future-of-mobility/electric-vehicle-trends-2030.html

[3] E. Outlook. (2020) Iea, paris. [Online]. Available: https://www.iea.org/reports/global-ev-outlook-202

[4] E. Commission and D.-G. for Energy, *Effect of electromobility on the power system and the integration of RES : study S13*. Publications Office, 2019.

[5] O. C. Onar and A. Khaligh, "Grid interactions and stability analysis of distribution power network with high penetration of plug-in hybrid electric vehicles," in *2010 Twenty-Fifth Annual IEEE Applied Power Electronics Conference and Exposition (APEC)*, 2010, pp. 1755–1762.

[6] A. Annamraju and S. Nandiraju, "Coordinated control of conventional power sources and phevs using jaya algorithm optimized pid controller for frequency control of a renewable penetrated power system," *Protection and Control of Modern Power Systems*, vol. 4, no. 1, pp. 1–13, 2019.

[7] N. B. Arias, S. Hashemi, P. B. Andersen, C. Træholt, and R. Romero, "Assessment of economic benefits for ev owners participating in the primary frequency regulation markets," *International Journal of Electrical Power & Energy Systems*, vol. 120, p. 105985, 2020.

[8] T. S. Ustun, J. Hashimoto, and K. Otani, "Impact of smart inverters on feeder hosting capacity of distribution networks," *IEEE Access*, vol. 7, pp. 163 526–163 536, 2019.

[9] L. Ibarra, A. Rosales, P. Ponce, A. Molina, and R. Ayyanar, "Overview of real-time simulation as a supporting effort to smart-grid attainment," *Energies*, vol. 10, no. 6, 2017. [Online]. Available: https://www.mdpi.com/1996-1073/10/6/817

[10] C. Edrington, M. Steurer, J. Langston, T. El-mezyani, and K. Schoder, "Role of power hardware in the loop in modeling and simulation for experimentation in power and energy systems," *Proceedings of the IEEE*, vol. 103, pp. 1–9, 10 2015.

[11] Z. Taylor, H. Akhavan-Hejazi, and H. Mohsenian-Rad, "Power hardware-in-loop simulation of grid-connected battery systems with reactive power control capability," 09 2017, pp. 1–6.

[12] N. Ninad, E. Apablaza-Arancibia, M. Bui, and J. Johnson, "Commercial pv inverter ieee 1547.1 ride-through assessments using an automated phil test platform," *Energies*, vol. 14, no. 21, 2021.

[13] F. Huerta, R. Tello, and M. Prodanovic, "Real-time power-hardware-in-the-loop implementation of variable-speed wind turbines," *IEEE Transactions on Industrial Electronics*, vol. PP, pp. 1–1, 11 2016.

[14] J.-H. Jung, "Real-time and power hardware-in-the-loop simulation of pem fuel cell stack system," *Journal of Power Electronics*, vol. 11, 03 2011.

[15] I. Jayawardana, C. Ho, and Y. Zhang, "A comprehensive study and validation of a power-hil testbed for evaluating grid-connected ev chargers," *IEEE Journal of Emerging and Selected Topics in Power Electronics*, vol. PP, pp. 1–1, 06 2021.

[16] L. De Herdt, A. Shekhar, Y. Yu, G. Chandra Mouli, J. Dong, and P. Bauer, "Power hardware-in-the-loop demonstrator for electric vehicle charging in distribution grids," in *2021 IEEE Transportation Electrification Conference & Expo (ITEC)*. United States: IEEE, 2021, pp. 679–683, green Open Access added to TU Delft Institutional Repository 'You share, we take care!' – Taverne project https://www.openaccess.nl/en/you-share-we-take-care Otherwise as indicated in the copyright section: the publisher is the copyright holder of this work and the author uses the Dutch legislation to make this work public.; 2021 IEEE Transportation Electrification Conference & Expo (ITEC) ; Conference date: 21-06-2021 Through 25-06-2021.

[17] M. Pokharel and C. N. M. Ho, "Stability analysis of power hardware-in-the-loop architecture with solar inverter," *IEEE Transactions on Industrial Electronics*, vol. 68, no. 5, pp. 4309–4319, 2020.

[18] A. Riccobono, A. Helmedag, A. Berthold, N. R. Averous, R. W. De Doncker, and A. Monti, "Stability and accuracy considerations of power hardware- in-the-loop test benches for wind turbines," *IFAC-PapersOnLine*, vol. 50, no. 1, pp. 10 977–10 984, 2017, 20th IFAC World Congress.

[19] E. Guillo-Sansano, M. H. Syed, A. J. Roscoe, G. M. Burt, and F. Coffele, "Characterization of time delay in power hardware in the loop setups," *IEEE Transactions on Industrial Electronics*, vol. 68, no. 3, pp. 2703–2713, 2020.

[20] O. R. Technologies. (2021) Rt lab online courses. preparing a simulink model for real time execution. [Online]. Available: $https://www.opal-rt.com/opal_tutorial/preparing-simulink-model-real-time-execution$

[21] *Technical Requirements for Connecting Small Scale PV (ssPV) Systems to Low Voltage Distribution Networks.*, BSN Std. 61 727, 2014.